NIH-PA Author Manuscript

Problem solving, working memory, and motor correlates of association and commissural fiber bundles in normal aging:

A quantitative fiber tracking study

Natalie M. Zahr[a,b], **Torsten Rohlfing**[b], **Adolf Pfefferbaum**[a,b], and **Edith V. Sullivan**[a,*]

a*Department of Psychiatry and Behavioral Sciences, Stanford University School of Medicine, 401 Quarry Road, Stanford, CA 94305-5723, USA*

b*Neuroscience Program, SRI International, Menlo Park, CA 94025, USA*

Abstract

Normal aging is accompanied by decline in selective cognitive and motor functions. A concurrent decline in regional white matter integrity, detectable with diffusion tensor imaging (DTI), potentially contributes to waning function. DTI analysis of white matter loci indicates an anterior-to-posterior gradient distribution of declining fractional anisotropy (FA) and increasing diffusivity with age. Quantitative fiber tracking can be used to determine regional patterns of normal aging of fiber systems and test the functional ramifications of the DTI metrics. Here, we used quantitative fiber tracking to examine age effects on commissural (genu and splenium), bilateral association (cingulate, inferior longitudinal fasciculus and uncinate), and fornix fibers in 12 young and 12 elderly healthy men and women and tested functional correlates with concurrent assessment of a wide range of neuropsychological abilities. Principal component analysis of cognitive and motor tests on which the elderly achieved significantly lower scores than the young group was used for data reduction and yielded three factors: Problem Solving, Working Memory, and Motor. Age effects - lower FA or higher diffusivity - in the elderly were prominent in anterior tracts, specifically, genu, fornix, and uncinate fibers. Differential correlations between FA or diffusivity in fiber tracts and scores on Problem Solving, Working Memory, or Motor factors provide convergent validity to the biological meaningfulness of the integrity of the fibers tracked. The observed pattern of relations supports the possibility that regional degradation of white matter fiber integrity is a biological source of age-related functional compromise and may have the potential to limit accessibility to alternative neural systems to compensate for compromised function.

Keywords

Fiber tracking; White matter; DTI; Cognition; Motor; Problem solving; Working memory; Age

Introduction

The search for brain mechanisms underlying complex cognitive, motor, and other behavioral functioning has shifted from single structures or loci to systems and circuits. Indeed, numerous functional MR imaging (fMRI) studies suggest that multiple brain regions are invoked to execute even the simplest psychomotor tasks. The systems conceptualization of brain functioning has logical appeal for understanding the neural bases of the highly variable and vastly complex behaviors characteristics of human performance and may serve to explain

*Corresponding author. Fax: +1 650 859 2743. *E-mail address:* edie@stanford.edu (E.V. Sullivan).

patterns of functional degradation typifying normal aging. With this shift comes the recognition of the relevance of connecting elements of brain circuitry and the possibility that disruption of the connections may be as effective as lesions in gray matter nodes in producing functional impairment. Until recently, the study of white matter bundles was restricted to postmortem analysis or slice-by-slice evaluation of structural MRI data. By contrast, magnetic resonance diffusion tensor imaging (DTI) has enabled noninvasive in vivo assessment of the integrity of brain connectivity by detecting the microenvironment of white matter (for reviews, Bammer et al., 2003; Le Bihan, 2003; Mori and Zhang, 2006; Sullivan and Pfefferbaum, 2007). DTI metrics applied to white matter regions include fractional anisotropy (FA), a measure of the orientationally restricted diffusion of water by fibers; apparent diffusion coefficient (ADC), a measure of water motility independent of orientation, commonly but not necessarily negatively correlated with FA within white matter samples (Chen et al., 2001; Engelter et al., 2000; Head et al., 2004; Helenius et al., 2002; Naganawa et al., 2003; Pfefferbaum et al., 2005; Pfefferbaum and Sullivan, 2003, 2005); longitudinal (axial) diffusivity ($\lambda 1$), reflecting axonal integrity; and transverse (radial) diffusivity (λt), reflecting myelin integrity (Song et al., 2002, 2005a; Sun et al., 2006a,b).

Typical DTI studies are based on analyses of intravoxel anisotropy in regionally restricted white matter samples but do not take advantage of DTI's ability to depict white matter systems through fiber tracking (Basser, 1998; Conturo et al., 1999; Jones et al., 1999; Lazar and Alexander, 2005; Masutani et al., 2003; Mori et al., 2002; Pajevic et al., 2002; Pierpaoli and Basser, 1996; Tang et al., 1997). Voxel-to-voxel connectivity between different brain regions is readily apparent on visual fiber tracking displays (Lehericy et al., 2004; Stieltjes et al., 2001; Xu et al., 2002), and measurements of FA and ADC along the length of a fiber bundle render estimates of its integrity. This approach, referred to as quantitative fiber tracking, is a statistical representation of the voxel-to-voxel coherence of MRI-detectable water diffusion in white matter. The validation of this statistical representation of white matter bundles by correlations with presumed function contribute to demonstrating that such measures are representative of underlying anatomy (Schmahmann et al., 2007).

An initial quantitative fiber tracking study of 10 normal, healthy elderly (72±5 years) and 10 young (29±5 years) adults revealed higher ADC, lower FA, and fewer fibers in anterior relative to posterior fiber bundles of the corpus callosum (Sullivan et al., 2006). A similar study described an age-related negative correlation with FA and an age-related positive correlation with mean diffusivity, measured using quantitative fiber tracking, in the genu and rostral body, but not splenium of the corpus callosum (Ota et al., 2006). In 120 healthy men and women spanning the adult age range from 20 to 81 years, the anterior-posterior gradient of age-related degradation of white matter endured: quantitative fiber tracking of major white matter cortical, subcortical, interhemispheric, and cerebellar systems demonstrated lower FA and higher diffusivity in anterior than posterior fibers (genu vs. splenium and frontal vs. occipital forceps). This pattern of lower FA and higher ADC in older than younger adults also pertained to superior versus inferior fiber systems (i.e., superior vs. inferior longitudinal fasciculi, superior vs. inferior cingulate bundle, Sullivan et al., in press). Stadlbauer et al. used quantitative fiber tracking to examine three different categories of fiber systems: association, callosal, and projection fibers (Stadlbauer et al., 2008a). Age-related declines in FA were greatest in association fibers and least in projection fibers, whereas mean diffusivity was significantly higher in the elderly in all three fiber systems. Because substructures of these fiber systems were not evaluated, the report was unable to comment on the anterior-posterior, superior-inferior age-related degradation gradient. In another study, quantitative fiber tracking identified age-related FA declines and ADC increases in the fornix but not cingulum (Stadlbauer et al., 2008b).

The in vivo elucidation of specific white matter tract anatomy combined with correlations with functional measures would allow for a better understanding of how brain fiber connectivity contributes to cognitive and motor function. To that end, we used quantitative fiber tracking to delineate multiple fiber systems throughout the brains of 12 young and 12 elderly, healthy men and women. Volunteers were administered a wide range of cognitive and motor tasks to validate DTI metrics by examining relations with performance of selective functions, categorized empirically as working memory, motor speed and dexterity, and problem solving. We expected an anterior-posterior and superior-inferior gradient of age-related white matter degradation with lower FA and higher diffusivity in the elderly than the young group. As previous study results indicate that both $\lambda 1$ and λt increase with age (Stadlbauer et al., 2008a,b; Sullivan et al., 2006, in press), we expected an age-related increase in both longitudinal and transverse diffusivity. Based on known anatomy (Table 1), we hypothesized that working memory would correlate with cingulum measures, and bimanual motor tasks with genu measurements. We also predicted that problem solving would show relationships with DTI metrics of a more widely distributed network of white matter (cf., Duncan and Owen, 2000).

Methods

Participants

With the exception of 5 elderly participants, this was a new cohort of subjects not included in our previous DTI studies (Pfefferbaum et al., in press, 2005, 2000). All 24 subjects in the present study participated in the current DTI acquisition protocol and a new neuropsychological test battery. Volunteers were 12 young (25.50 ± 4.34 years, range=19-33 years) and 12 elderly (77.67 ± 4.94 years, range=67-84 years), right-handed, nonsmoking healthy men and women, recruited from the local community (Table 2). Each subject provided signed, informed consent to participate in this study, as approved by the Institutional Review Boards of SRI International and Stanford University. The Structured Clinical Interview for the Diagnostic and Statistical Manual (DSM) IV, administered by a trained research psychologist, was used to detect DSM-IV diagnoses or medical conditions that can affect brain functioning (e.g., diabetes, head injury, epilepsy, uncontrolled hypertension, radiation/chemotherapy) or preclude MR study (e.g., pacemakers).

The two age groups did not differ significantly in education or estimated general intelligence (NART IQ; Table 2). The elderly had a higher socioeconomic status (SES, Hollingshead, 1975), but scored lower than the young on the Dementia Rating Scale (DRS, cutoff for dementia <124 out of 144, Mattis, 1988), although well-within the normal range of published values for healthy elderly individuals living in the community (e.g., 137.48 ± 5.18, Vitaliano et al., 1984). The significantly greater body mass index (BMI; slightly overweight, i.e., BMI between 25 and 29.9 kg/m^2) of the elderly than the young was close to the mean BMI calculated from 5,200 subjects participating in the cardiovascular health study (26.3 ± 3.9 kg/m2, Janssen et al., 2005). Although the elderly had significantly higher systolic blood pressure than the young group, they were all in the pre-hypertensive range (i.e., between 120 and 139 mmHg, Chobanian et al., 2003). The participants in this study also underwent MR spectroscopic evaluation (Zahr et al., 2008).

Neuropsychological assessment

Psychomotor testing, designed to assess a wide range of cognitive and motor functions to question whether regional DTI metrics had functional significance, included measures of reaction time, verbal and nonverbal fluency, working memory, set-shifting, rule formation, upper and lower limb motor function. Tests, their neurocognitive significance, and the scores used for analysis are listed in Table 3. Each test score was standardized by z-transformation to

produce a mean score of 0 and a standard deviation of 1; scores were multiplied by-1 for tests in which high raw scores were indicative of worse performance (e.g., reaction time). For tests on which the elderly achieved significantly ($p \leq .05$) lower scores than the young group (Table 4; t-tests and Mann-Whitney U tests), z-scores for each test were submitted to a principal component analysis (PCA; orthogonal transformation varimax solution), which yielded three factors with eigenvalues ≥ 2. The resulting test clusters were theoretically meaningful. Consequently, each test measure was sorted into one of the three identified factors, together accounting for 71% of the variance in neuropsychological test performance: Working Memory, Motor, or Problem Solving. Composite scores for each factor were calculated as the mean of the standardized z-scores of the tests identified within a factor.

DTI and MRI acquisition

DTI data were acquired with an 8-channel head coil at 3.0 T after higher-order (nonlinear) shimming. DTI and FSE data were collected with the same slice locations: DTI (2D echo-planar, TR=7300 ms, TE=86.6 ms, thickness=2.5 mm, skip=0, locations=62, b=0 (5 NEX)+15 noncollinear diffusion directions b=860s/mm^2 (2 NEX)+15 opposite polarity noncollinear diffusion directions b=860s/mm^2 (2 NEX), FOV=240 mm, x-dim=96, y-dim=96, reconstructed to 128×128, 4030 total images); FSE (2D axial, TR=7850 ms, TE=17/102 ms, thickness=2.5 mm, skip=0, locations=62). T1-weighted SPGR (3D axial IR-prep, TR=6.5 ms, TE=1.6 ms, thick=1.25 mm, skip=0, locations=124) images were aligned, such that two 1.25 mm SPGR slices subtended each 2.5 mm thick FSE/DTI slice. A fieldmap was generated from a gradient recalled echo sequence.

DTI analysis

DTI quantification was preceded by eddy current correction on a slice-by-slice basis using within-slice registration, which took advantage of the symmetry of the opposing polarity acquisition (Bodammer et al., 2004) and also allowed for compensation of the diffusion effect created by the imaging gradients (Neeman et al., 1991), reducing the data to 15 non-collinear diffusion-weighted images per slice for tensor computation. Using the field maps, B_0-field inhomogeneity-induced geometric distortion in the eddy current-corrected images was corrected with PRELUDE (Phase Region Expanding Labeller for Unwrapping Discrete Estimates, Jenkinson, 2003) and FUGUE (FMRIB's Utility for Geometrically Unwarping EPIs, Jenkinson, 2001). Maps of the apparent diffusion coefficient (ADC) were calculated, each being a sum of three elements of the diffusion tensor. Solving the equations with respect to ADCxx, ADCxy, etc. yielded the elements of the diffusion tensor. The diffusion tensor was then diagonalized, yielding eigenvalues $\lambda_1, \lambda_2, \lambda_3$, and eigenvectors that define the predominant diffusion orientation. Based on the eigenvalues, FA and ADC were calculated on a voxel-by-voxel basis (Basser and Jones, 2002; Basser and Pierpaoli, 1998; Pierpaoli and Basser, 1996). These "native space" DTI data were used for fiber tracking.

To achieve common anatomical coordinates across subjects, SPGR data for each subject were aligned with a brain template made from these 24 subjects ("SRI24 atlas", Rohlfing et al., 2008) with group-wise nonrigid registration (Learned-Miller, 2006; Rohlfing and Maurer, 2003). Each subject's FA data were reformatted into common space using the transformation computed between the SRI24 space and that subject's SPGR data, concatenated with the transformation from subject SPGR to subject DTI space. From the reformatted FA maps from all subjects, a group average FA image was then created. Fiber tract seed points were identified on the group average FA image with single point landmarks in 3 dimensions on axial or coronal slices. The commissural fibers (genu and splenium) were identified at their maximum in the midline; the fornix was also identified in the midline. Bilateral association tracts were identified with anterior-posterior locations: inferior longitudinal fasciculus, cingulum bundle (superior, posterior and inferior portions), and uncinate fasciculus. For fiber tracking, the target and

sources were then mapped to the corresponding locations on the native basis images for each subject with a numerical inversion of the transformation previously used to reformat the individual FA maps into SRI24 space. The tensor matrix, targets, and sources were passed to the fiber tracking routine in native space, the output of which was a 3D graphic of the fiber paths plus a table of all point locations along each fiber with local DTI metrics (FA, ADC, etc.).

Fiber tracking

Fiber tracking was performed with the software by Gerig et al. (Gerig et al., 2005) based on the method of Mori and colleagues (Mori and van Zijl, 2002; Xu et al., 2002, 1999). Fiber tracking parameters included white matter extraction threshold (minimum FA) of .17, minimum fiber length of 37.5 mm, maximum fiber length of 187.5 mm, fiber tracking threshold of .125, and maximum voxel-to-voxel coherence minimum transition smoothness threshold of .80 (~37° maximum deviation between fiber segments from neighboring voxels), with no limit on the number of fibers.

Identified fibers were required to originate in source voxels and pass through target voxels. In common (atlas) space, each landmark was dilated with a morphological operator to produce a 5 mm cube as the fiber-tracking target. Sources were 3 mm thick planes: a) 5 mm bilateral to commissural targets, b) 5 mm anterior and 5 mm posterior to association and fornix targets. The mean FA and ADC of all voxels comprising each fiber, for all fibers, were determined.

After fiber detection the fiber locations were transformed back to common standard coordinates for display and further analysis. Fiber tracking on the group-average FA image in common space identified 5 association fibers (superior, posterior, and inferior cingulate, uncinate fasciculus and inferior longitudinal fasciculus), 2 commissural fibers (genu and splenium), and the fornix (Fig. 1). For each region, mean FA, ADC, longitudinal diffusivity ($\lambda 1 = \lambda_1$) and transverse diffusivity ($\lambda t = [\lambda_2 + \lambda_3]/2$) for each fiber bundle were the units of analysis.

Statistical analysis

Primary analyses were based on group-by-fiber tract and group-by-factor analysis of variance (ANOVA); where appropriate, Green-house-Geiser (GG) correction was applied, and only group effects and interactions involving group effects were of interest to this analysis. Follow-up group differences were determined by t-tests and confirmed by Mann-Whitney U tests with the prediction that the elderly group would have lower FA, higher diffusivity, and poorer test performance than the young group. In another set of analysis, we examined whether individual fiber tract DTI metrics (FA and ADC) were predictive of test performance (PCA factors) using simple linear regressions. Only Spearman Rank correlations enduring a family-wise Bonferroni correction for 8 comparisons (5 bilateral, 2 commissural, and fornix measures), for which 1-tailed p-values≤0.012 were significant were considered for further analysis. The relationships among age, PCA factors, and selected DTI fiber metric variables were calculated with hierarchical regression. The percentage of variance in performance in each PCA factor explained by a) age and b) selected DTI metrics were evaluated. Also calculated were the percentage of c) variance in age-PCA factor relations attenuated by selected DTI metrics and d) variance in DTI metrics-PCA factor relations attenuated by age (Anstey et al., 1997).

Results

Group differences in DTI metrics

FA and ADC—Separate repeated measures ANOVAs examining genu and splenium FA or ADC in the young and elderly revealed group effects ($F(1,22)=14.5$, $p=.001$; ADC $F(1,22)=26.89$, $p=.0001$) and group-by-region interactions, indicating that relative to the young group,

the elderly group tended to have disproportionately lower FA ($F(1,22)=2.82$, $p=.1071$) and had higher ADC ($F(1,22)=4.44$, $p=.0468$) in the genu than splenium. Follow-up t-tests confirmed these effects, indicating lower FA in the genu ($t(22)=6.15$, $p=.0001$) and higher ADC in the genu ($t(22)=-5.4$, $p=.0001$) and splenium ($t(22)=-3.37$, $p=.0028$) of the elderly than young groups (Fig. 2).

A repeated-measures ANOVA for FA, involving two groups, two hemispheres, and the five bilateral association fiber tracts, yielded a group effect ($F(1,22)=10.839$, $p=.0033$) and group-by-hemisphere interaction ($F(1,22)=4.939$, $p=.0368$ GG). FA was lower in the elderly than young group in the left superior cingulate ($t(22)=2.45$, $p=.0229$), left inferior cingulate ($t(22)=2.63$, $p=.0151$), left inferior longitudinal fasciculus ($t(22)=2.26$, $p=.034$), and left ($t(22)=2.93$, $p=.0078$) and right ($t(22)=2.85$, $p=.0093$) uncinate.

A repeated-measures ANOVA for ADC, involving two groups, two hemispheres, and the five bilateral association fiber tracts, yielded a group effect ($F(1,22)=7.316$, $p=.0129$) and a trend for a group-by-tract interaction ($F(4,88)=2.388$, $p=.0734$ GG), but no other interactions involving group. Follow-up analysis, based on average values of the two hemispheres, indicated that ADC was higher in the elderly than young group in the uncinate fasciculi ($t(22)=4.82$, $p=.0001$) and showed a trend to be higher in the superior cingulum ($t(22)=1.99$, $p=.0587$).

A t-test demonstrated lower FA ($t(22)=7.05$, $p=.0001$) and higher ADC ($t(22)=8.32$, $p=.0001$) in the fornix of the elderly than young groups (Fig. 2). The fornix was analyzed separately because, whereas the genu and splenium are both commissural fibers, and the cingulum, inferior longitudinal fasciculus, and the uncinate fasciculus are bilaterally distributed association fibers, the anatomy of the fornix makes it difficult to categorize as either commissural or association, as it has properties of both.

λ1 and λ*t*—Separate repeated-measures ANOVAs examining genu and splenium λ1 or λt in the young and elderly revealed group effects (λ1 $F(1,22)=11.66$, $p=.0025$; λt $F(1,22)=37.12$, $p=.0001$). A significant group-by-region interaction indicated that the elderly group had disproportionately higher λt ($F(1,22)=7.27$, $p=.0132$) in the genu than splenium. Follow-up t-tests indicated higher diffusivity component values in the elderly than young group in the genu (λ1 $(22)=3.14$, $p=.0048$; λt $t(22)=7.58$, $p=.0001$) and splenium (λ1 $t(22)=2.56$, $p=.0177$; λt $t(22)=3.11$, $p=.0051$; Fig. 2).

A repeated-measures ANOVA for λ1, involving two groups, two hemispheres, and five fiber tracts, yielded a group-by-tract interaction ($F(4,88)=3.227$, $p=.0337$ GG) but no group effect ($F(1,22)=.806$, p=.3791) and no significant interactions involving group and hemisphere. Follow-up analysis, based on average values of the two hemispheres, indicated that λ1 was higher in the elderly than young group in the uncinate ($t(22)=3.95$, $p=.0007$).

A repeated-measures ANOVA for λt, involving two groups, two hemispheres, and five fiber tracts, yielded a group effect ($F(1,22)=14.548$, $p=.0009$) but no significant interactions involving group. Follow-up analysis indicated that λt was higher in the elderly than young group in the superior cingulum ($t(22)=2.81$, $p=.0101$) and uncinate ($t(22)=4.94$, $p=.0001$).

In the fornix, t-tests indicated higher λ1 ($t(22)=7.13$, $p=.0001$) and higher λt ($t(22)=8.85$, $p=.0001$) in the elderly than young groups (Fig. 2).

Group differences in neuropsychological performance

Table 4 presents mean raw scores±standard deviations for performance on cognitive and motor tests, p-values from two group t-tests, and confirmatory Mann-Whitney *U* tests. With a t-test,

all tests with the exception of phonological fluency, digit forward and backward, fine finger movements, and comprehensive trail making showed significant age effects. With a Mann-Whitney U test, the balance task was additionally not significantly different between groups. The tests showing age-related compromise in performance with a Mann-Whitney U test were submitted to PCA and categorized into 3 factors as demonstrated in Table 4. A two group by three testfactor ANOVA yielded a group effect ($F(1,22)=43.610$, $p=.0001$). Follow-up group comparisons of the PCA factors revealed that the elderly group achieved lower scores than the young group on Working Memory ($t(22)=4.363$, $p=.0002$), Motor ($t(22)=4.557$, $p=.0002$), and Problem Solving ($t(22)=4.75$, $p=.0001$) composite scores.

Correlations between FA and ADC and neuropsychological factors scores

Simple regression analysis included all subjects to test relations between each of the three performance factors and FA and ADC for each of the eight fiber tracts (left and right hemisphere DTI values were averaged where appropriate). A family-wise Bonferroni correction was calculated, representing the eight fiber tracts measured, resulting in a 1-tailed p value (given the directional nature of our predictions) of .012 for $\alpha=.05$.

Working Memory correlations (Table 5, Fig. 3) with genu FA, and fornix FA and ADC were significant with family-wise Bonferroni correction and confirmed with Spearman Rank Order correlation. Table 6 shows the total variance in the Working Memory composite explained by age and the individual DTI metrics that correlated with Working Memory. Also included is the proportion of variance contributed by age after each DTI metric was considered and the proportion of variance accounted for by each DTI metric after age was considered. When tested individually, age and the 3 selected DTI metrics contributed significantly to the variance in Working Memory performance. However, when the relationships between age and the DTI metrics were considered together, neither age nor the DTI metrics explained a significant proportion of the variance in Working Memory. Each DTI metric alone attenuated the age-related variance in performance on Working Memory by at least 82%, and the three metrics together attenuated the age-Working Memory relationship by 99% (Table 7).

The Motor measure (Table 5, Fig. 4) correlated by simple regression with genu FA and ADC, splenium ADC, fornix FA and ADC, superior cingulum FA and ADC, inferior cingulum FA, inferior longitudinal fasciculus FA, and uncinate fasciculus FA and ADC. With a Spearman Rank Order test, correlations were similar; the only difference was that inferior longitudinal fasciculus ADC instead of FA correlated with the Motor composite. With a family-wise Bonferroni correction on the Spearman's correlations, the fibers that remained significantly correlated with the Motor composite were genu, fornix, and uncinate fasciculus FA and ADC, and splenium ADC. The total variance in Motor performance explained by age, each DTI metric alone, age after each DTI metric, and each DTI metric after age is presented in Table 8. Again, when tested individually, age and each DTI metric alone explained a significant proportion of the variance in Motor performance. With a Bonferroni correction, age remained a significant contributor to the variance in Motor performance after splenium ADC and uncinate fascicules FA were considered (i.e., age remained significant when each of these fiber metrics was entered prior to age). Conversely, when age was entered prior to uncinate fasciculus FA, there remained a significant contribution by the uncinate fasciculus FA measurement to the variance in Motor performance. However, when genu ADC, fornix FA, or fornix ADC were entered before age, age no longer explained a significant proportion of the variance in Motor performance. Genu ADC, fornix FA, and fornix ADC each attenuated the relationship between Motor performance and age by at least 84% (Table 9). Further, although the 7 fiber metrics together reduced the age-related variance in Motor performance by 84%, the 3 fiber metrics tested (i.e., genu FA, fornix FA and ADC) together reduced the age related variance by over 99% suggesting that they account for a large portion of the age-related variance in Motor performance.

The Problem Solving composite (Table 5, Fig. 5) correlated with parametric and nonparametric tests and Bonferroni correction with genu and fornix FA and ADC. When tested individually, age and each of the 4 DTI metrics explained a significant proportion of the variance in Problem Solving performance. None of the fiber metrics explained all of the age-related variance in Problem Solving, as there was a significant contribution of age to Problem Solving after entry of each of each fiber measure (Table 10). When age was entered prior to each DTI metric, there was no significant remaining contribution of the relevant DTI metric to the variance. Together, these results suggest that none of the fiber metrics explained a significant proportion of the variance in Problem Solving performance independent of age. Genu ADC and fornix FA each reduced the age-Problem Solving relationship by 77%, while all 4 metrics together attenuated the relationship by 96% (Table 11).

Discussion

Anterior fiber systems (genu, uncinate fasciculus, and fornix) were more sensitive than posterior systems (splenium, cingulum, and inferior longitudinal fasciculus) to age, regardless of the DTI metric (e.g., FA, ADC, $\lambda 1$, or λt) used for the age comparison. We also provide evidence for associations between microstructural connectivity integrity and cognitive and motor performance in healthy young and elderly men and women with robust correlations identified between the cognitive and motor composite test scores and genu and fornix FA and ADC. Demonstration of predictable relationships provides validation of DTI fiber tracking metrics of specific white matter systems as representative of underlying anatomy

Age effects

DTI metrics—Quantitative fiber tracking revealed aging effects in FA, ADC, $\lambda 1$, or λt in six of the eight fiber systems measured. A current consensus of DTI studies, whether based on region-of-interest, voxel-based morphometry, or quantitative fiber tracking, indicates that with advancing age, FA declines and ADC increases in anterior brain regions disproportionately more than posterior regions (Head et al., 2004; Madden et al., 2004; O'Sullivan et al., 2001; Pfefferbaum et al., 2005; Pfefferbaum and Sullivan, 2003; Salat et al., 2005). Using quantitative fiber tracking, we have also demonstrated more consistent age effects on superior compared with inferior fiber systems (Sullivan et al., in press). In the current study, the age-related pattern of low FA and high ADC in anterior-posterior and superior-inferior gradients persisted, with age effects most prominent in the genu, fornix, and uncinate fibers. In all three fiber systems, the pattern of aging effects on DTI metrics were similar: the decrease in FA and increase in ADC were accompanied by increases in both $\lambda 1$ and λt, suggesting that lower FA and higher ADC were due to the increases in longitudinal and transverse diffusivity. In the splenium, an increase in $\lambda 1$, λt, and ADC were observed. Age-related DTI metric differences in the cingulum were only evident in the superior region (i.e., the most anterior portion), where FA was lower and λt higher in the elderly than young. Age effects on all four DTI metrics in the fornix, but on only two in the superior cingulum, and none in the posterior or inferior cingulate bundle regions comports with a recent study demonstrating that the cingulum is relatively resistant to age, whereas the fornix is not (Stadlbauer et al., 2008b). The inferior longitudinal fasciculus revealed age-related compromise detectable with FA in the current study and ADC in our previous study (Sullivan et al., in press); in neither study was longitudinal or transverse diffusivity related to age.

Exceptionally high diffusion values for the fornix have previously been noted (Fujiwara et al., 2008; Stadlbauer et al., 2008b). Indeed, in our 1.5 T quantitative fiber tracking study, by far the highest diffusivity measures were in the fornix (Sullivan et al., in press). A potential explanation is that the fornix is surrounded by cerebral spinal fluid (CSF), which might increase the effects of partial voluming (i.e., the inclusion of CSF rather than white matter in the voxel),

thereby contaminating diffusivity measures; however, the criterion of a minimum of FA=.17 in the fiber tracking routine mitigates against the unwanted influence of CSF in the targeted white matter voxel. Further, although ADC in the fornix was about double that of any other fiber system, FA in the fornix was well within range of other fibers.

Pathological studies have demonstrated that an increase in λt accompanies breakdown of myelin (Beaulieu et al., 1996; Glenn et al., 2003; Gulani et al., 2001; Ono et al., 1995; Pierpaoli et al., 2001b; Schwartz and Hackney, 2003; Song et al., 2003, 2005b). Advancing age, as shown by postmortem study, is also associated with myelin breakdown (Bartzokis et al., 2004; Feldman and Peters, 1998; Marner et al., 2003; Meier-Ruge et al., 1992; Peters and Sethares, 2002; Peters et al., 2001). Thus, age-related increases in λt are consistent with age-related modifications to myelin. In contrast to the current results, pathological studies have demonstrated that $\lambda 1$ decreases in acute axonal injury, specifically in distal sites where injury (e.g., stroke, ischemia) induces Wallerian degeneration (Schwartz and Hackney, 2003; Song et al., 2003; Sun et al., 2006b; Thomalla et al., 2004). Despite evidence for axonal damage with age (Sandell and Peters, 2003), older age has also been associated with loss of tissue organization, increases in extra-axonal fluid, or other alterations in the extracellular space surrounding axons (Aboitiz et al., 1996; Meier-Ruge et al., 1992; Nusbaum et al., 2001; Sen and Basser, 2005), all of which can increase diffusivity, contributing to the increase in $\lambda 1$ seen in normal aging (Stadlbauer et al., 2008a,b; Sullivan et al., 2006, in press). This pattern also occurs in primary stroke regions (in contrast to distal regions) where resolution of necrosis is followed by water accumulation in interstitial spaces and formation of cystic spaces filled by cerebral spinal fluid (Pierpaoli et al., 2001a). Thus, while $\lambda 1$ is assumed to represent axonal modification, a decrease or increase in the measure can be informative about the underlying processes, with a decrease likely representing axonal degeneration, and an increase likely signifying fluid accumulation in regions around the axon.

Neuropsychological factors scores related to DTI metrics and age

Normal aging is accompanied by declines in selective cognitive and motor functions and frontally based executive functions are especially vulnerable to undesirable effects of advancing age (but see Greene et al., 2008; Raz and Rodrigue, 2006; Stuss and Alexander, 2000). The current study demonstrates that the elderly performed significantly worse than the young on PCA-derived Working Memory, Motor, and Problem Solving domains, the latter of which included multiple tasks drawing on frontally-based brain systems (Robbins et al., 1998).

Functional correlates of the DTI measures provide convergent validity to the biological meaningfulness of the tracked fiber loci and metrics. Here, performance in the Working Memory domain was related to the integrity of the genu and fornix. The genu links anterior right and left hemispheres, including prefrontal regions. Given the dependence of Working Memory on the integrity of prefrontal regions (Badre, 2008), the correlations between Working Memory and the genu would be expected. The fornix is the primary link between the hippocampus and the mammillary bodies and anterior thalamic nuclei, principal components of Papez circuit (Papez, 1937). In rodents, the fornix and the hippocampus each have been shown to be required for successful performance on a spatial working memory task, the eight-arm radial maze (Sziklas and Petrides, 2002).

Seven of the eight fiber system metrics reported herein correlated with performance on the Motor composite. Four fiber system correlations with the Motor factor composite were robust as they endured both the nonparametric evaluation and the Bonferroni correction: the genu (FA and ADC), splenium (ADC), fornix (FA and ADC), and uncinate fasciculus (FA and ADC). This set of correlations suggests that a complex network of systems is involved in integrating multiple functions for execution of the speed and dexterity required to accomplish the motor

tasks of this study. Our motor measure included tasks requiring visual search, comprehension (CANTAB Motor, and CANTAB Big/Little Circle), and learning (CANTAB Big/Little Circle), which likely involve the recruitment of visuospatial attention systems, such as the parietal cortices (Ehrsson et al., 2002; Guye et al., 2003; Tuch et al., 2005), visuospatial context systems, such as the temporal cortices (Kwok and Buckley, 2006), and even decision making centers in superior frontal regions (Gallea et al., 2005; Karagulle Kendi et al., 2008), which together would necessitate the integrity of commissural fibers as well as the fornix and uncinate fasciculi to promote effective and efficient performance.

The Problem Solving composite correlated with genu and fornix FA and ADC. Interhemispheric projections through the genu connecting bilateral prefrontal cortical sites (de Lacoste et al., 1985; Hofer and Frahm, 2006) may contribute to optimal performance on "executive tasks" by enabling coordinated functioning from both hemispheres in conditions, such as successful aging, where unilateral functioning is suboptimal (Cabeza et al., 2002). Recent DTI studies using region-of-interest measures report that FA in the genu of the corpus callosum of cocaine-dependent subjects correlated with greater impulsivity (measured with the Barratt impulsiveness scale) and reduced discriminability (measured with an Immediate and Delayed Memory task, Devanand et al., 2006). In healthy, elderly subjects, reduced perceptual-motor speed correlated with FA in the genu (Bucur et al., 2007). The splenium is composed of interhemispheric fibers coursing between several cortical areas, including parietal regions (de Lacoste et al., 1985; Hofer and Frahm, 2006), implicated in attentional shifting (Gurd et al., 2002) and visuospatial information transfer (Suzuki et al., 1998). A recent DTI study in adolescents demonstrates the importance of splenium integrity (FA) to Rey-Osterrieth Complex Figure copy accuracy, WASI Vocabulary, and WRAT-3 reading scores (Fryer et al., 2008), tasks that include attentional, visuospatial, and linguistic integration. Furthermore, we have previously shown, in alcohol dependent individuals, correlations between performance on matrix reasoning, a task challenging visuospatial abilities, and splenium DTI metrics (Pfefferbaum et al., 2006). Lesions of the fornix can disrupt declarative episodic (Gaffan, 2005; Kuroki et al., 2006), associative (Gaffan et al., 2002), and working memory (Sziklas and Petrides, 2002). In addition to its linkage to sites serving primarily mnemonic functions (e.g., Papez circuit), the fornix projects to the anterior thalamus (Paxinos, 1990) and nucleus accumbens (Kelley and Domesick, 1982), placing it in a strategic position to integrate complex functions that draw on these additional gray matter regions and likely necessary for successful performance on the tasks included in the Problem Solving domain.

Limitations

A limitation of the current study is that principal component analysis data reduction blurs the components that comprise the factors, potentially obscuring relevant correlations between neuropsychological test performance and fiber system metrics. However, given the 16 neuropsychological test scores acquired and the combined 32 DTI metrics for the 8 fiber systems, data reduction was a necessary step to conduct the correlational search in our modest sample size. Another limitation of this study was the small sample size and the bimodal distribution of ages, so that our exploration of brain structure-function relationships in these two groups of healthy men and women were founded on a non-continuous variable (age) for the correlational analyses. Further, correlational analyses cannot imbue causality, regardless of the complexity of the correlational approach used and further, neuropsychological correlates of white matter fiber systems merely reflect the connections between gray matter nodes that are the primary brain regions responsible for executing actions. An ideal study would account for gray matter volume in relevant regions of interest and would analyze the specificity of brain structural measures (gray matter volume vs. white matter diffusion properties) as predictors of selective performance measures. Given our current understanding that systems and circuits linking multiple brain regions are invoked to execute even the simplest psychomotor tasks, it

is possible that performance would be mediated more by the integrity of specific white matter systems than by regional cortical gray matter volumes.

Conclusions

We have collected on a 3T system DTI data adequately robust to conduct quantitative fiber tracking in selective bilateral association and commissural fiber bundles and to observe an anterior-posterior and superior-inferior gradient effects of age-related degradation. The DTI-functional correlations are consistent with the possibility of regional degradation of white matter fiber integrity as a biological source of age-related functional compromise and provide validation of DTI metrics of white matter fiber tracts as representative of underlying anatomy.

Acknowledgments

References

Aboitiz F, Rodriguez E, Olivares R, Zaidel E. Age-related changes in fibre composition of the human corpus callosum: sex differences. Neuroreport 1996;7:1761–1764. [PubMed: 8905659]

Aggleton JP, Brown MW. Episodic memory, amnesia, and the hippocampal-anterior thalamic axis. Behav. Brain Sci 1999;22:425–444. [PubMed: 11301518]discussion 444-489

Anstey KJ, Lord SR, Williams P. Strength in the lower limbs, visual contrast sensitivity, and simple reaction time predict cognition in older women. Psychol. Aging 1997;12:137–144. [PubMed: 9100274]

Badre D. Cognitive control, hierarchy, and the rostro-caudal organization of the frontal lobes. Trends Cogn. Sci 2008;12:193–200. [PubMed: 18403252]

Bammer R, Acar B, Moseley ME. In vivo MR tractography using diffusion imaging. Eur. J. Radiol 2003;45:223–234. [PubMed: 12595107]

Barbas H, Pandya DN. Topography of commissural fibers of the prefrontal cortex in the rhesus monkey. Exp. Brain Res 1984;55:187–191. [PubMed: 6745350]

Bartzokis G, Sultzer D, Lu PH, Nuechterlein KH, Mintz J, Cummings JL. Heterogeneous age-related breakdown of white matter structural integrity: implications for cortical "disconnection" in aging and Alzheimer's disease. Neurobiol. Aging 2004;25:843–851. [PubMed: 15212838]

Basser, PJ. Fiber-Tractography via Diffusion Tensor MRI (DT-MRI) (abs); Proceedings of the International Society of Magnetic Resonance in Medicine, 6th Meeting; 1998; p. 1226

Basser PJ, Pierpaoli C. A simplified method to measure the diffusion tensor from seven MR images. Magn. Reson. Med 1998;39:928–934. [PubMed: 9621916]

Basser PJ, Jones DK. Diffusion-tensor MRI: theory, experimental design and data analysis- a technical review. NMR Biomed 2002;15:456–467. [PubMed: 12489095]

Beaulieu C, Does MD, Snyder RE, Allen PS. Changes in water diffusion due to Wallerian degeneration in peripheral nerve. Magn. Reson. Med 1996;36:627–631. [PubMed: 8892217]

Bertram, E.; Moore, K. An Atlas of the Human Brain and Spinal Cord. Williams & Wilkins; Baltimore: 1982.

Bodammer N, Kaufmann J, Kanowski M, Tempelmann C. Eddy current correction in diffusion-weighted imaging using pairs of images acquired with opposite diffusion gradient polarity. Magn. Reson. Med 2004;51:188–193. [PubMed: 14705060]

Borkowski JG, Benton AL, Spreen O. Word fluency and brain damage. Neuropsychologia 1967;5:135–140.

Bucur B, Madden DJ, Spaniol J, Provenzale JM, Cabeza R, White LE, Huettel SA. Age-related slowing of memory retrieval: contributions of perceptual speed and cerebral white matter integrity. Neurobiol. Aging. 2007

Cabeza R, Anderson ND, Locantore JK, McIntosh AR. Aging gracefully: compensatory brain activity in high-performing older adults. NeuroImage 2002;17:1394–1402. [PubMed: 12414279]

Chen ZG, Li TQ, Hindmarsh T. Diffusion tensor trace mapping in normal adult brain using single-shot EPI technique. A methodological study of the aging brain. Acta Radiol 2001;42:447–458. [PubMed: 11552881]

Chobanian AV, Bakris GL, Black HR, Cushman WC, Green LA, Izzo JL Jr. Jones DW, Materson BJ, Oparil S, Wright JT Jr. Roccella EJ. Seventh report of the Joint National Committee on Prevention, Detection, Evaluation, and Treatment of High Blood Pressure. Hypertension 2003;42:1206–1252. [PubMed: 14656957]

Conturo T, Lori N, Cull T, Akbudak E, Snyder A, Shimony J, McKinstry R, Burton H, Raichle M. Tracking neuronal fiber pathways in the living human brain. Proc. Natl. Acad. Sci. U. S. A 1999;96:10422–10427. [PubMed: 10468624]

Corkin, S.; Growdon, JH.; Sullivan, EV.; Nissen, MJ.; Huff, FJ. Assessing treatment effects from a neuropsychological perspective. In: Poon, L., editor. Handbook of Clinical Memory Assessment in Older Adults. American Psychological Association; Washington DC: 1986. p. 156-167.

de Lacoste M, Kirkpatrick J, Ross E. Topography of the human corpus callosum. J. Neuropathol. Exp. Neurol 1985;44:578–591. [PubMed: 4056827]

Desmond JE, Gabrieli JD, Wagner AD, Ginier BL, Glover GH. Lobular patterns of cerebellar activation in verbal working-memory and finger-tapping tasks as revealed by functional MRI. J. Neurosci 1997;17:9675–9685. [PubMed: 9391022]

Devanand DP, Habeck CG, Tabert MH, Scarmeas N, Pelton GH, Moeller JR, Mensh BD, Tarabula T, Van Heertum RL, Stern Y. PET network abnormalities and cognitive decline in patients with mild cognitive impairment. Neuropsychopharmacology 2006;31:1327–1334. [PubMed: 16292330]

Duncan J, Owen AM. Common regions of the human frontal lobe recruited by diverse cognitive demands. Trends Neurosci 2000;23:475–483. [PubMed: 11006464]

Ehrsson HH, Kuhtz-Buschbeck JP, Forssberg H. Brain regions controlling nonsynergistic versus synergistic movement of the digits: a functional magnetic resonance imaging study. J. Neurosci 2002;22:5074–5080. [PubMed: 12077202]

Engelter ST, Provenzale JM, Petrella JR, DeLong DM, MacFall JR. The effect of aging on the apparent diffusion coefficient of normal-appearing white matter. Am. J. Roentgenol 2000;175:425–430. [PubMed: 10915688]

Feldman ML, Peters A. Ballooning of myelin sheaths in normally aged macaques. J. Neurocytol 1998;27:605–614. [PubMed: 10405027]

Fryer SL, Frank LR, Spadoni AD, Theilmann RJ, Nagel BJ, Schweinsburg AD, Tapert SF. Microstructural integrity of the corpus callosum linked with neuropsychological performance in adolescents. Brain Cogn. 2008

Fujiwara S, Sasaki M, Kanbara Y, Inoue T, Hirooka R, Ogawa A. Feasibility of 1.6-mm isotropic voxel diffusion tensor tractography in depicting limbic fibers. Neuroradiology 2008;50:131–136. [PubMed: 17938897]

Gaffan D. Neuroscience. Widespread cortical networks underlie memory and attention. Science 2005;309:2172–2173. [PubMed: 16195447]

Gaffan D, Easton A, Parker A. Interaction of inferior temporal cortex with frontal cortex and basal forebrain: double dissociation in strategy implementation and associative learning. J Neurosci 2002;22:7288–7296. [PubMed: 12177224]

Gallea C, de Graaf JB, Bonnard M, Pailhous J. High level of dexterity: differential contributions of frontal and parietal areas. Neuroreport 2005;16:1271–1274. [PubMed: 16056123]

Gerig, G.; Corouge, I.; Vachet, C.; Krishnan, KR.; MacFall, JR. Quantitative analysis of diffusion properties of white matter fiber tracts: a validation study; 13th Proceedings of the International Society for Magnetic Resonance in Medicine; Miami, FL. 2005; Abstract no. 1337

Glenn OA, Henry RG, Berman JI, Chang PC, Miller SP, Vigneron DB, Barkovich AJ. DTI-based three-dimensional tractography detects differences in the pyramidal tracts of infants and children with congenital hemiparesis. J. Magn. Reson. Imaging 2003;18:641–648. [PubMed: 14635148]

Greene CM, Braet W, Johnson KA, Bellgrove MA. Imaging the genetics of executive function. Biol Psychol 2008;79:30–42. [PubMed: 18178303]

Gulani V, Webb AG, Duncan ID, Lauterbur PC. Apparent diffusion tensor measurements in myelin-deficient rat spinal cords. Magn. Reson. Med 2001;45:191–195. [PubMed: 11180424]

Gurd JM, Amunts K, Weiss PH, Zafiris O, Zilles K, Marshall JC, Fink GR. Posterior parietal cortex is implicated in continuous switching between verbal fluency tasks: an fMRI study with clinical implications. Brain 2002;125:1024–1038. [PubMed: 11960893]

Guye M, Parker GJ, Symms M, Boulby P, Wheeler-Kingshott CA, Salek-Haddadi A, Barker GJ, Duncan JS. Combined functional MRI and tractography to demonstrate the connectivity of the human primary motor cortex in vivo. Neuroimage 2003;19:1349–1360. [PubMed: 12948693]

Head D, Buckner RL, Shimony JS, Williams LE, Akbudak E, Conturo TE, McAvoy M, Morris JC, Snyder AZ. Differential vulnerability of anterior white matter in nondemented aging with minimal acceleration in dementia of the Alzheimer type: evidence from Diffusion Tensor Imaging. Cerebral Cortex 2004;14:410–423. [PubMed: 15028645]

Helenius J, Soinne L, Perkio J, Salonen O, Kangasmaki A, Kaste M, Carano RA, Aronen HJ, Tatlisumak T. Diffusion-weighted MR imaging in normal human brains in various age groups. Am. J. Neuroradiol 2002;23:194–199. [PubMed: 11847041]

Hofer S, Frahm J. Topography of the human corpus callosum revisited-comprehensive fiber tractography using diffusion tensor magnetic resonance imaging. Neuroimage 2006;32:989–994. [PubMed: 16854598]

Hollingshead, A. Four-factor index of social status. Yale University, Department of Sociology; New Haven, CT: 1975.

Janssen I, Katzmarzyk PT, Ross R. Body mass index is inversely related to mortality in older people after adjustment for waist circumference. J. Am. Geriatr. Soc 2005;53:2112–2118. [PubMed: 16398895]

Jenkinson, M. Improved unwarping of EPI volumes using regularised B_0 Maps (abs); Seventh International Conference on Functional Mapping of the Human Brain; 2001;

Jenkinson M. A fast, automated, N-dimensional phase unwrapping algorithm. J. Magn. Reson. Med 2003;49:193–197.

Jones D, Simmons A, Williams S, Horsfield M. Non-invasive assessment of axonal fiber connectivity in the human brain via diffusion tensor MRI. Magn. Reson. Med 1999;42:37–41. [PubMed: 10398948]

Karagulle Kendi AT, Lehericy S, Luciana M, Ugurbil K, Tuite P. Altered diffusion in the frontal lobe in Parkinson disease. AJNR Am. J. Neuroradiol 2008;29:501–505. [PubMed: 18202242]

Kelley AE, Domesick VB. The distribution of the projection from the hippocampal formation to the nucleus accumbens in the rat: an anterograde-and retrograde-horseradish peroxidase study. Neuroscience 1982;7:2321–2335. [PubMed: 6817161]

Kuroki N, Kubicki M, Nestor PG, Salisbury DF, Park HJ, Levitt JJ, Woolston S, Frumin M, Niznikiewicz M, Westin CF, Maier SE, McCarley RW, Shenton ME. Fornix integrity and hippocampal volume in male schizophrenic patients. Biol. Psychiatry 2006;60:22–31. [PubMed: 16406249]

Kwok SC, Buckley MJ. Fornix transection impairs exploration but not locomotion in ambulatory macaque monkeys. Hippocampus 2006;16:655–663. [PubMed: 16779812]

Lazar M, Alexander AL. Bootstrap white matter tractography (BOOT-TRAC). NeuroImage 2005;24:524–532. [PubMed: 15627594]

Le Bihan D. Looking into the functional architecture of the brain with diffusion MRI. Nat. Rev. Neurosci 2003;4:469–480. [PubMed: 12778119]

Learned-Miller EG. Data driven image models through continuous joint alignment. IEEE Trans. Pattern. Anal. Mach. Intell 2006;28:236–250. [PubMed: 16468620]

Lehericy S, Ducros M, Van de Moortele PF, Francois C, Thivard L, Poupon C, Swindale N, Ugurbil K, Kim DS. Diffusion tensor fiber tracking shows distinct corticostriatal circuits in humans. Ann. Neurol 2004;55:522–529. [PubMed: 15048891]

Madden DJ, Whiting WL, Huettel SA, White LE, MacFall JR, Provenzale JM. Diffusion tensor imaging of adult age differences in cerebral white matter: relation to response time. NeuroImage 2004;21:1174–1181. [PubMed: 15006684]

Marner L, Nyengaard JR, Tang Y, Pakkenberg B. Marked loss of myelinated nerve fibers in the human brain with age. J. Comp. Neurol 2003;462:144–152. [PubMed: 12794739]

Masutani Y, Aoki S, Abe O, Hayashi N, Otomo K. MR diffusion tensor imaging: recent advance and new techniques for diffusion tensor visualization. Eur. J. Radiol 2003;46:53–66. [PubMed: 12648802]

Mattis, S. Dementia Rating Scale (DRS) professional manual. Psychological Assessment Resources, Inc.; Odessa, FL: 1988.

Meier-Ruge W, Ulrich J, Bruhlmann M, Meier E. Age-related white matter atrophy in the human brain. Ann. N.Y. Acad. Sci 1992;673:260–269. [PubMed: 1485724]

Mori S, Kaufmann WE, Davatzikos C, Stieltjes B, Amodei L, Fredericksen K, Pearlson GD, Melhem ER, Solaiyappan M, Raymond GV, Moser HW, van Zijl PC. Imaging cortical association tracts in the human brain using diffusion-tensor-based axonal tracking. Magn. Reson. Med 2002;47:215–223. [PubMed: 11810663]

Mori S, van Zijl PC. Fiber tracking: principles and strategies - a technical review. NMR Biomed 2002;15:468–480. [PubMed: 12489096]

Mori S, Zhang J. Principles of diffusion tensor imaging and its applications to basic neuroscience research. Neuron 2006;51:527–539. [PubMed: 16950152]

Mufson EJ, Pandya DN. Some observations on the course and composition of the cingulum bundle in the rhesus monkey. J. Comp. Neurol 1984;225:31–43. [PubMed: 6725639]

Naganawa S, Sato K, Katagiri T, Mimura T, Ishigaki T. Regional ADC values of the normal brain: differences due to age, gender, and laterality. Eur. Radiol 2003;13:6–11. [PubMed: 12541104]

Neeman M, Freyer JP, Sillerud LO. A simple method for obtaining cross-termfree images for diffusion anisotropy studies in NMR microimaging. Magn. Reson. Med 1991;21:138–143. [PubMed: 1943671]

Newcombe, F. Missile Wounds of the Brain: A Study of Psychological Deficits. Oxford University Press; London: 1969.

Nusbaum AO, Tang CY, Buchsbaum MS, Wei TC, Atlas SW. Regional and global changes in cerebral diffusion with normal aging. Am. J. Neuroradiol 2001;22:136–142. [PubMed: 11158899]

O'Sullivan M, Jones D, Summers P, Morris R, Williams S, Markus H. Evidence for cortical "disconnection" as a mechanism of age-related cognitive decline. Neurology 2001;57:632–638. [PubMed: 11524471]

Ono J, Harada K, Takahashi M, Maeda M, Ikenaka K, Sakurai K, Sakai N, Kagawa T, Fritz-Zieroth B, Nagai T, et al. Differentiation between dysmyelination and demyelination using magnetic resonance diffusional anisotropy. Brain Res 1995;671:141–148. [PubMed: 7728526]

Orsini A, Chiacchio L, Cinque M, Cocchiaro C, Schiappa O, Grossi D. Effects of age, education and sex on two tests of immediate memory: a study of normal subjects from 20 to 99 years of age. Percept. Mot. Skills 1986;63:727–732. [PubMed: 3808855]

Ota M, Obata T, Akine Y, Ito H, Ikehira H, Asada T, Suhara T. Age-related degeneration of corpus callosum measured with diffusion tensor imaging. NeuroImage 2006;31:1445–1452. [PubMed: 16563802]

Pajevic S, Aldroubi A, Basser PJ. A continuous tensor field approximation of discrete DT-MRI data for extracting microstructural and architectural features of tissue. J. Magn. Reson 2002;154:85–100. [PubMed: 11820830]

Papez JW. A proposed mechanism of emotion. Arch. Neurol 1937;38:725–743.

Paxinos, G. The Human Nervous System. Paxinos, G., editor. Academic Press; San Diego, CA: 1990.

Peters A, Sethares C. Aging and the myelinated fibers in prefrontal cortex and corpus callosum of the monkey. J. Comp. Neurol 2002;442:277–291. [PubMed: 11774342]

Peters A, Sethares C, Killiany RJ. Effects of age on the thickness of myelin sheaths in monkey primary visual cortex. J. Comp. Neurol 2001;435:241–248. [PubMed: 11391644]

Petrides M, Pandya DN. Association fiber pathways to the frontal cortex from the superior temporal region of the rhesus monkey. J. Comp. Neurol 1988;273:52–66. [PubMed: 2463275]

Pfefferbaum A, Adalsteinsson E, Rohlfing T, Sullivan EV. Diffusion tensor imaging of deep gray matter brain structures: effects of age and iron concentration. Neurobiol. Aging. in press

Pfefferbaum A, Sullivan EV. Increased brain white matter diffusivity in normal adult aging: relationship to anisotropy and partial voluming. Magn. Reson. Med 2003;49:953–961. [PubMed: 12704779]

Pfefferbaum A, Sullivan EV. Disruption of brain white matter microstructure by excessive intracellular and extracellular fluid in alcoholism: evidence from diffusion tensor imaging. Neuropsychopharmacology 2005;30:423–432. [PubMed: 15562292]

Pfefferbaum A, Adalsteinsson E, Sullivan EV. Frontal circuitry degradation marks healthy adult aging: evidence from diffusion tensor imaging. NeuroImage 2005;26:891–899. [PubMed: 15955499]

Pfefferbaum A, Adalsteinsson E, Sullivan EV. Dysmorphology and microstructural degradation of the corpus callosum: Interaction of age and alcoholism. Neurobiol. Aging 2006;27:994–1009. [PubMed: 15964101]

Pfefferbaum A, Sullivan EV, Hedehus M, Lim KO, Adalsteinsson E, Moseley M. Age-related decline in brain white matter anisotropy measured with spatially corrected echo-planar diffusion tensor imaging. Magn. Reson. Med 2000;44:259–268. [PubMed: 10918325]

Pierpaoli C, Basser PJ. Towards a quantitative assessment of diffusion anisotropy. Magn. Reson. Med 1996;36:893–906. [PubMed: 8946355]

Pierpaoli C, Barnett A, Pajevic S, Chen R, Penix L, Virta A, Basser PJ. Water diffusion changes in Wallerian degeneration and their dependence on white matter architecture. NeuroImage 2001a; 13:1174–1185. [PubMed: 11352623]

Pierpaoli C, Barnett A, Pajevic S, Chen R, Penix LR, Virta A, Basser P. Water diffusion changes in Wallerian degeneration and their dependence on white matter architecture. Neuroimage 2001b; 13:1174–1185. [PubMed: 11352623]

Raz N, Rodrigue KM. Differential aging of the brain: patterns, cognitive correlates and modifiers. Neurosci. Biobehav. Rev 2006;30:730–748. [PubMed: 16919333]

Robbins TW, James M, Owen AM, Sahakian BJ, Lawrence AD, McInnes L, Rabbitt PM. A study of performance on tests from the CANTAB battery sensitive to frontal lobe dysfunction in a large sample of normal volunteers: implications for theories of executive functioning and cognitive aging.Cambridge Neuropsychological Test Automated Battery. J. Int. Neuropsychol. Soc 1998;4:474–490. [PubMed: 9745237]

Rohlfing T, Maurer CR. Nonrigid image registration in shared-memory multi-processor environments with application to brains, breasts, and bees. IEEE Trans. Inf. Technol. Biomed 2003;7:16–25. [PubMed: 12670015]

Rohlfing T, Zahr NM, Sullivan EV, Pfefferbaum A. The SRI24 multi-channel brain atlas: construction and applications medical imaging 2008: image processing. Proc. SPIE 2008;6914:691409.

Ruff RM, Light RH, Evans RW. The Ruff Figural Fluency Test: a normative study with adults. Developmental Neuropsychology 1987;3:37–51.

Salat DH, Tuch DS, Greve DN, van der Kouwe AJW, Hevelone ND, Zaleta AK, Rosen BR, Fischl B, Corkin S, Rosas HD, Dale AM. Age-related alterations in white matter microstructure measured by diffusion tensor imaging. Neurobiol. Aging 2005;26:1215–1227. [PubMed: 15917106]

Sandell JH, Peters A. Disrupted myelin and axon loss in the anterior commissure of the aged rhesus monkey. J. Comp. Neurol 2003;466:14–30. [PubMed: 14515238]

Schmahmann JD, Pandya DN, Wang R, Dai G, D'Arceuil HE, de Crespigny AJ, Wedeen VJ. Association fibre pathways of the brain: parallel observations from diffusion spectrum imaging and autoradiography. Brain 2007;130:630–653. [PubMed: 17293361]

Schwartz ED, Hackney DB. Diffusion-weighted MRI and the evaluation of spinal cord axonal integrity following injury and treatment. Exp. Neurol 2003;184:570–589. [PubMed: 14769351]

Seltzer B, Pandya DN. The distribution of posterior parietal fibers in the corpus callosum of the rhesus monkey. Exp. Brain Res 1983;49:147–150. [PubMed: 6861933]

Sen PN, Basser PJ. A model for diffusion in white matter in the brain. Biophys. J 2005;89:2927–2938. [PubMed: 16100258]

Smith SR, Servesco AM, Edwards JW, Rahban R, Barazani S, Nowinski LA, Little JA, Blazer AL, Green JG. Exploring the validity of the Comprehensive Trail Making Test. Clin. Neuropsychol 2007:1–12. [PubMed: 17366273]

Song SK, Sun SW, Ramsbottom MJ, Chang C, Russell J, Cross AH. Dysmyelination revealed through MRI as increased radial (but unchanged axial) diffusion of water. NeuroImage 2002;17:1429–1436. [PubMed: 12414282]

Song SK, Sun SW, Ju WK, Lin SJ, Cross AH, Neufeld AH. Diffusion tensor imaging detects and differentiates axon and myelin degeneration in mouse optic nerve after retinal ischemia. Neuroimage 2003;20:1714–1722. [PubMed: 14642481]

Song SK, Yoshino J, Le TQ, Lin SJ, Sun SW, Cross AH, Armstrong RC. Demyelination increases radial diffusivity in corpus callosum of mouse brain. NeuroImage 2005a;26:132–140. [PubMed: 15862213]

Song SK, Yoshino J, Le TQ, Lin SJ, Sun SW, Cross AH, Armstrong RC. Demyelination increases radial diffusivity in corpus callosum of mouse brain. Neuroimage 2005b;26:132–140. [PubMed: 15862213]

Stadlbauer A, Salomonowitz E, Strunk G, Hammen T, Ganslandt O. Age-related degradation in the central nervous system: assessment with diffusion-tensor imaging and quantitative fiber tracking. Radiology 2008a;247:179–188. [PubMed: 18292477]

Stadlbauer A, Salomonowitz E, Strunk G, Hammen T, Ganslandt O. Quantitative diffusion tensor fiber tracking of age-related changes in the limbic system. Eur. Radiol 2008b;18:130–137. [PubMed: 17701181]

Stieltjes B, Kaufmann WE, van Zijl PC, Fredericksen K, Pearlson GD, Solaiyappan M, Mori S. Diffusion tensor imaging and axonal tracking in the human brainstem. NeuroImage 2001;14:723–735. [PubMed: 11506544]

Stuss DT, Alexander MP. Executive functions and the frontal lobes: a conceptual view. Psychol. Res 2000;63:289–298. [PubMed: 11004882]

Sullivan EV, Pfefferbaum A. Neuroradiological characterization of normal adult aging. Br. J. Radiol 2007;60:S99–S108. [PubMed: 18445750]

Sullivan EV, Adalsteinsson E, Pfefferbaum A. Selective age-related degradation of anterior callosal fiber bundles quantified in vivo with fiber tracking. Cerebral Cortex 2006;16:1030–1039. [PubMed: 16207932]

Sullivan EV, Rohlfing T, Pfefferbaum A. Quantitative fiber tracking of lateral and interhemispheric white matter systems in normal aging: relations to timed performance. Neurobiol. Aging. in press

Sun SW, Liang HF, Le TQ, Armstrong RC, Cross AH, Song SK. Differential sensitivity of in vivo and ex vivo diffusion tensor imaging to evolving optic nerve injury in mice with retinal ischemia. Neuroimage 2006a;32:1195–1204. [PubMed: 16797189]

Sun SW, Liang HF, Trinkaus K, Cross AH, Armstrong RC, Song SK. Noninvasive detection of cuprizone induced axonal damage and demyelination in the mouse corpus callosum. Magn. Reson. Med 2006b;55:302–308. [PubMed: 16408263]

Suzuki K, Yamadori A, Endo K, Fujii T, Ezura M, Takahashi A. Dissociation of letter and picture naming resulting from callosal disconnection. Neurology 1998;51:1390–1394. [PubMed: 9818866]

Sziklas V, Petrides M. Effects of lesions to the hippocampus or the fornix on allocentric conditional associative learning in rats. Hippocampus 2002;12:543–550. [PubMed: 12201639]

Tang, CY.; Lu, D.; Wei, TC.; Spiegel, J.; Atlas, SW.; Buchsbaum, MS. Image processing techniques for the eigenvectors of the diffusion tensor (abs); International Society for Magnetic Resonance in Medicine 5th Meeting; 1997; p. 2054

Thomalla G, Glauche V, Koch MA, Beaulieu C, Weiller C, Rother J. Diffusion tensor imaging detects early Wallerian degeneration of the pyramidal tract after ischemic stroke. Neuroimage 2004;22:1767–1774. [PubMed: 15275932]

Trites, RL. Neuropsychological Test Manual. Royal Ottawa Hospital; Ontario, Canada: 1990. The Grooved Pegboard Test.

Tuch DS, Salat DH, Wisco JJ, Zaleta AK, Hevelone ND, Rosas HD. Choice reaction time performance correlates with diffusion anisotropy in white matter pathways supporting visuospatial attention. Proc. Natl. Acad. Sci. U. S. A 2005;102:12212–12217. [PubMed: 16103359]

Vitaliano PP, Breen AR, Albert MS, Russo J, Prinz PN. Memory, attention, and functional status in community-residing Alzheimer type dementia patients and optimally healthy aged individuals. J. Gerontol 1984;39:58–64. [PubMed: 6690588]

Xu D, Mori S, Solaiyappan M, van Zijl PC, Davatzikos C. A framework for callosal fiber distribution analysis. NeuroImage 2002;17:1131–1143. [PubMed: 12414255]

Xue R, van Zijl PC, Crain BJ, Solaiyappan M, Mori S. In vivo three-dimensional reconstruction of rat brain axonal projections by diffusion tensor imaging. Magn. Reson. Med 1999;42:1123–1127. [PubMed: 10571934]

Zahr NM, Mayer D, Pfefferbaum A, Sullivan EV. Low striatal glutamate levels underlie cognitive decline in the elderly: Evidence from in vivo molecular spectroscopy. Cereb. Cortex 2008;18:2241–2250. [PubMed: 18234683]
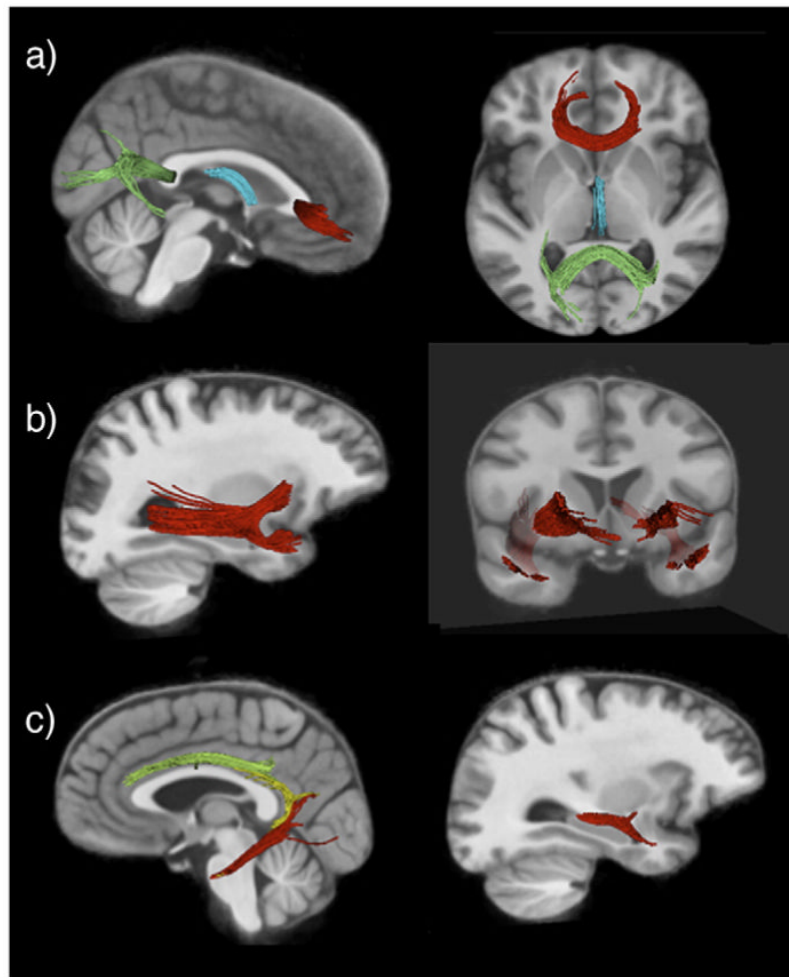
Fig. 1.
Fiber tracts were identified on the group-average FA image in common space. (a) Sagittal (left) and axial (right) views of the genu (red), splenium (green), and fornix (blue). (b) Sagittal (left) and coronal (right) views of the uncinate fasciculus. (c) Sagittal views of the cingulum (left; superior, green; posterior, yellow; inferior, red) and inferior longitudinal fasciculus (right).
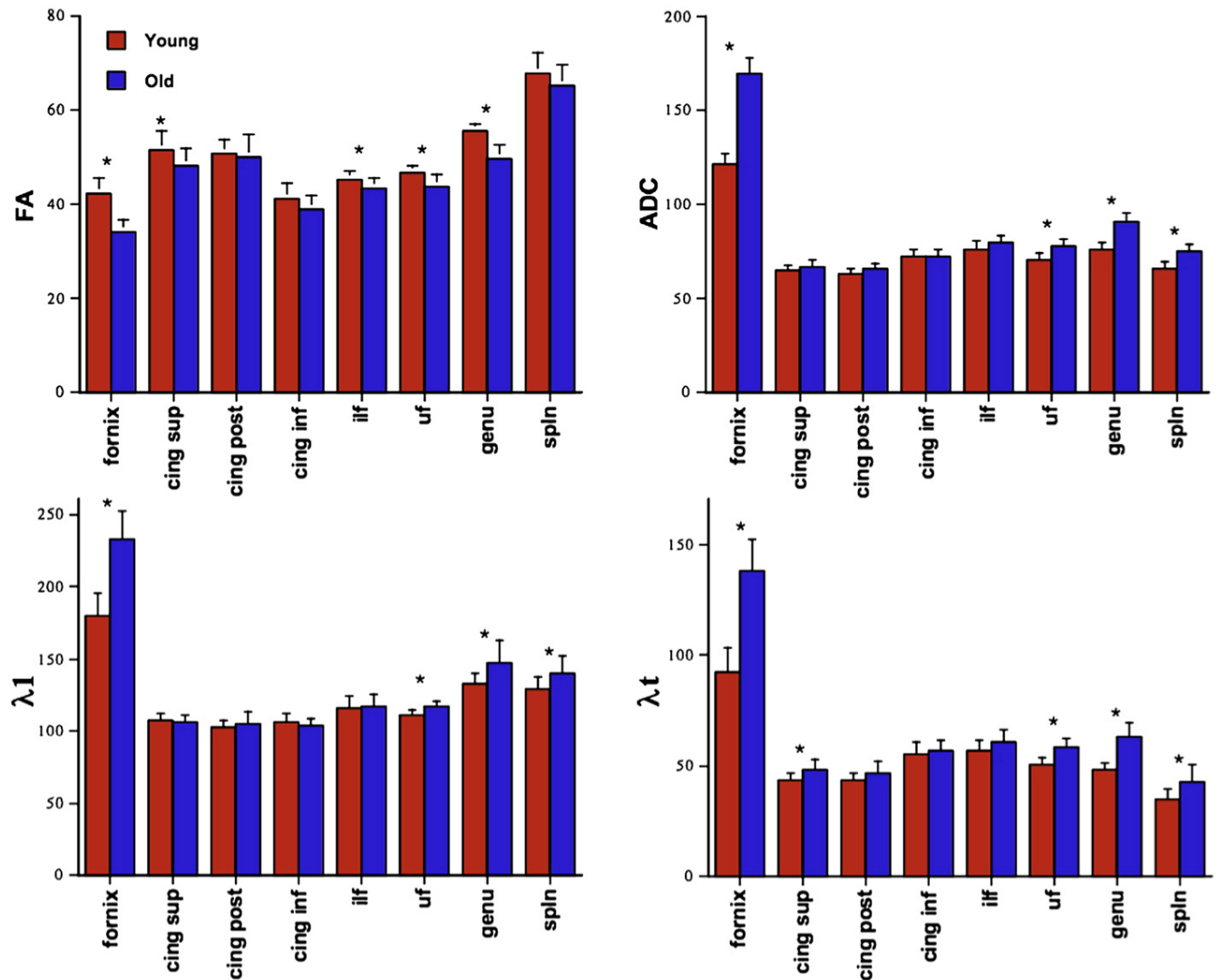
Fig. 2.
Mean±S.D. for FA, ADC, λ1, and λt for young (red) and elderly (blue) subjects for each fiber bundle. *$p \leq .05$ *t*-test. With a Mann-Whitney *U* test, superior cingulum FA is not significantly different between groups.
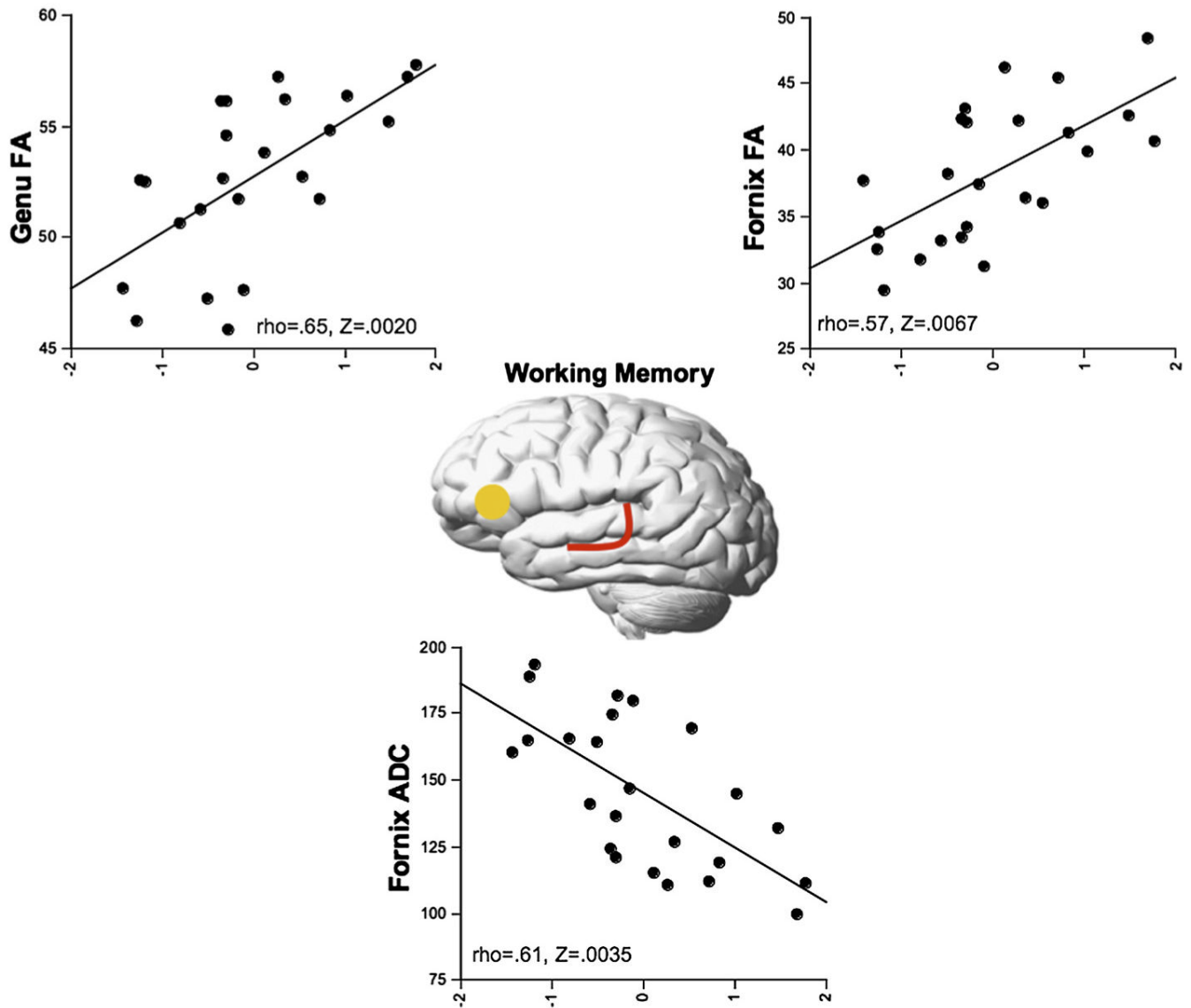
Fig. 3.
Correlations (Spearman Rank and Bonferroni corrected) between the Working Memory domain isolated using PCA and DTI metrics (FA and ADC) by tract.
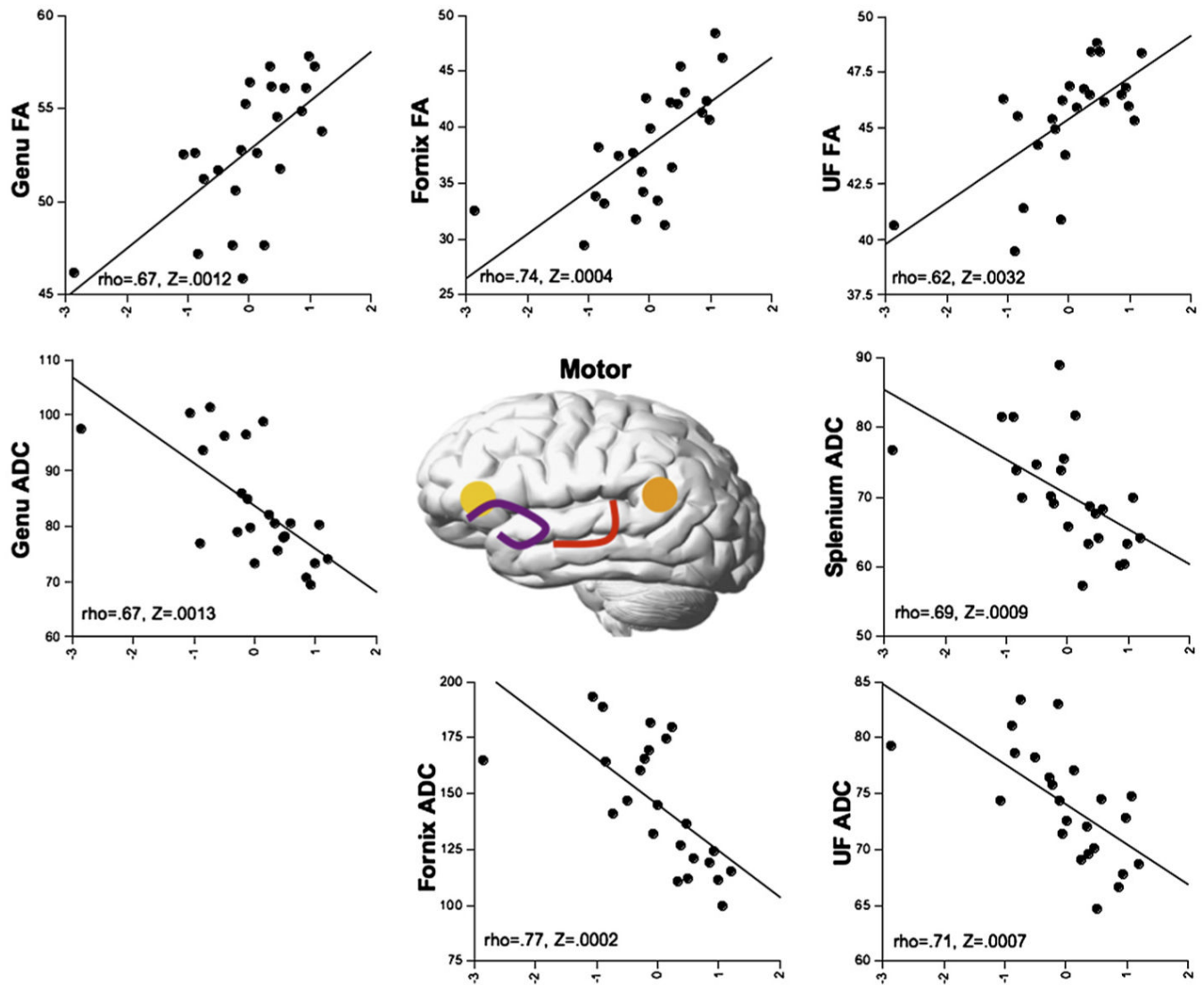
Fig. 4.
Correlations (Spearman Rank and Bonferroni corrected) between the Motor domain isolated
using PCA and DTI metrics (FA and ADC) by tract.
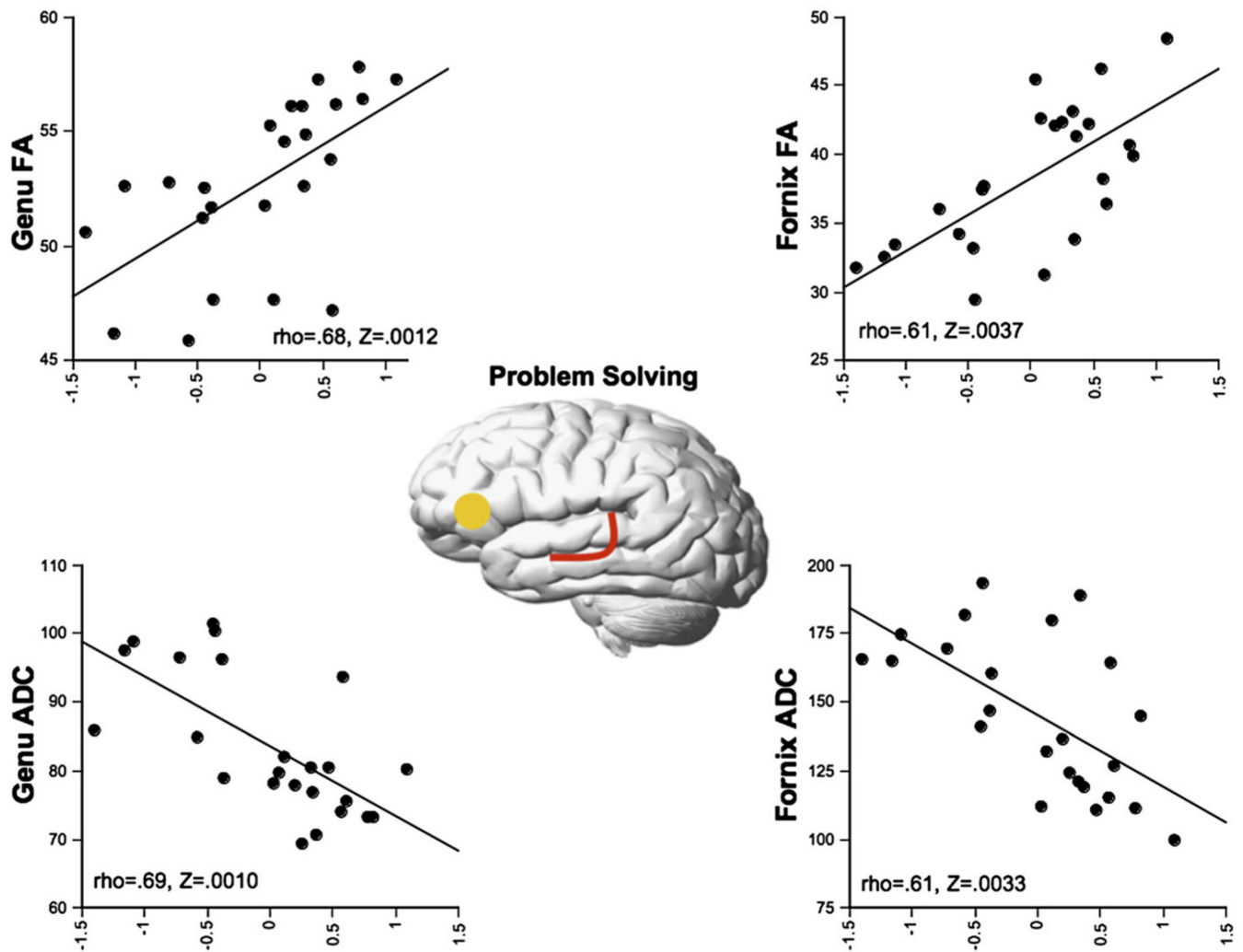
Fig. 5.
Correlations (Spearman Rank and Bonferroni corrected) between the Problem Solving domain isolated using PCA and DTI metrics (FA and ADC) by tract.

Table 1

Characterization of fiber tracts

Fiber tracts	Conneting	With	References
Commissural			
Genu	Anterior right and left hemispheres	(Prefrontal/premotor/supplementary motor)	(Barbas and Pandya, 1984)
Splenium	Posterior right and left hemispheres	(Parietal/temporal/occipital)	(Seltzer and Pandya, 1983)
Fornix	Hippocampus	Mammilary bodies/hypoyhalamus/anterior thalamic nuclei	(Aggleton and Brown, 1999)
Association			
Cingulum	Thalamus/cingulate gyrus/prefrontal+parietal corticles	Retrospenial cortex/parahippocampal gyrus/presubiculum	(Mufson and Pandya, 1984)
Uncinate fasciculus	Orbital/medial/lateral frontal cortices	Superior temporal gyrus	(Petrides and Pandya, 1988)
Inferior longitudinal fasciculus	Occipital cortices	Temporal lobes	(Bertram and Moore, 1982)

Table 2

Group demographics: means, standard deviations, and ranges

	Young (6 M, 6 F)	Elderly (6 M, 6 F)	p value[a]
Age (years)	25.50±4.34 (19-33)	77.67±4.94 (67-84)	<0.0001
Education (years)	16.25±2.18 (14-21)	17.08±1.98 (14-21)	0.337
NART IQ	113.67±5.66 (102-121)	118.17±5.59 (107-126)	0.063
DRS	141.42±2.57 (136-144)	137.25±4.71 (130-143)	0.013
BMI	23.08±2.98 (19-29)	26.64±4.55 (21-37)	0.034
Systolic BP (mm Hg)	114.00±16.16 (93-143)	135.92±21.84 (108-178)	0.011
Diastolic BP (mm Hg)	68.58±8.46 (59-88)	75.42±11.65 (60-96)	0.114

[a]
t-tests.

Table 3

Neupsychological tests

Test	Scope	Test scores	Reference
Phonological Fluency	Phonological retrieval/working memory	Total words produced for letters, F+A+S	(Borkowski et al., 1967)
Digit Forward	Immediate numeric span	Total recalled numbers, forward	(Orsini et al., 1986)
Digit Backward	Immediate numeric span	Total recalled numbers, backward	(Orsini et al., 1986)
Blocks Forward	Immediate visual span	Total recalled blocks, forward	(Orsini et al., 1986)
Sternberg[*]	Verbal working memory	High load (6 letters) RT - low load (1 letter) RT; stimulus present	(Desmond et al., 1997)
Fine Finger Movements	Upper limb motor dexterity	Total turns, average right and left, unimanual and bimanual	(Corkin et al., 1986)
Grooved Pegboard[*]	Upper limb motor dexterity	Total time, average right and left hands	(Trites, 1977)
Cantab: Motor[*]	Visual search/comrehension/motor	Reaction time (RT)	http://www.camcog.com
Cantab: Big/LittleCircle[*]	""+Learning/reversal learning	Reaction time (RT)	http://www.camcog.com
Comprehensive Trail Making Test[*]	Visual search/flexibility/complex sequencing	Mean t-score last 2 trials - mean t-score for first 3 trials	(Smith et al., 2007)
Semantic Fluency	Semantic retrieval/working memory	Average category words produced in 3 categories[a]	(Newcombe, 1969)
Figural Fluency	Rule acquisition/visuospatial working	Total unique designs across five trials	(Ruff et al., 1987)
Blocks Backward	Immediate visual span	Total recalled blocks, backward	(Orsini et al., 1986)
Cantab: Stockings of Cambridge	Spatial planning/motor control	# of problems solved in minimum moves	http://www.camcog.com
Cantab: Intra-Extra Dimensional Shift[*]	Rule acquisition/attentional set shifting	# of trial to complete stage 8 - mean # trials to complete stages 6+7	http://www.camcog.com
Balance+Problem Solving Task[*b]	Dual processing: lower limb motor/problem solving	Average sway path eyes open and closed across 18 trials	

[*] Higher scores=worse performance.

[a] Animals, inanimate objects, and birds/colors.

[b] The force platform experiment is employed while subjects stand, without shoes, in the center of a Kistler Force Platform (model 9284; Amherst, NY). Subjects are tested with their feet together, arms relaxed at their sides, and eyes either open or closed. In the single processing condition, subjects simply stand quietly on the platform. A secondary task is given to produce a dual processing condition. In the dual task condition, subjects listen, through speakers mounted on either side of the force platform, to sets of pre-recorded digit strings (9 total). Strings are spoken in 4.5 s epochs, followed by .5 s intervals for the subjects' response. In the easier condition, subjects hear three digits and two operands followed by a correct (66%) or incorrect (33%) answer (e.g. 2+5-3=4; 3-1+8=11) to which they must say "yes" or "no" to each problem. In the harder condition, subjects must additionally respond "odd" or "even" in response to the answer given. Each condition is repeated 3 times; the score is the average of the three trials.

Table 4

Mean±SD of raw scores on neuropsychologicalmeasures

	Young (*n*=12)	Elderly (*n*=12)	*p* Value[a]	*Z* score[b]
Phonological Fluency	40.33±11.74	39.75±12.90	.9088	1.00
Digit Forward	8.75±2.05	8.92±2.11	.8462	.7693
Digit Backward	7.25±2.49	7.00±2.37	.8036	.7702
Blocks Forward	9.33±1.23	7.33±1.07	*.0003*	*.0011* } WM
Sternberg[*]	259.10±155.67	435.06±97.36	*.0031*	*.0094*
Fine Finger Movements[c]	76.73±17.55	68.28±19.32	.2839	.1239
Grooved Pegboard[*]	67.12±9.33	96.29±17.09	*.0001*	*.0003* } MOT
CANTAB: Motor[*]	774.50±156.22	1061.07±157.04	*.0118*	*.0022*
CANTAB: Big/LittleCircle[*]	704.88±107.47	902.1±157.04	*.0016*	*.0018*
Comprehensive Trail Making Test	2.53±7.31	8.5±11.67	.1472	.1259
Balance÷Problem Solving Task[*c]	74.10±20.81	117.24±62.28	*.0339*	.0966
Semantic Fluency	22.28±3.14	17.19±4.21	*.0029*	*.0055* } PS
Figural Fluency	100.25±13.44	80.33±9.76	*.0004*	*.0007*
Blocks Backward	9.00±1.28	7.33±1.67	*.0118*	*.0186*
Stockings of Cambridge	10.25±1.42	8.17±2.21	*.0118*	*.0209*
Intra-Extra Dimensional Shift Task[*]	5.08±5.9	22.62±16.58	*.0023*	*.0021*

[a] *t*-tests

[b] Mann-Whitney *U* test corrected for ties

[c] *n*=11 for elderly

[*] higher scores = worse performance, WM = Working Memory, MOT = Motor, PS = Problem Solving.

Table 5

r and p^a and Rho and Z^b values for correlations between PCA factors and DTI metrics

	Working memory				Motor				Problem solving			
	r	p	Rho	Z	r	p	Rho	Z	r	p	Rho	z
Genu												
FA	.63	.0010	.65	.0020	.64	.0008	.67	.0012	.60	.0019	.68	.0012
ADC	.43	.0349	.44	.0331	.67	.0003	.67	.0013	.67	.0004	.69	.0010
Splenium												
FA	.02	.9293	.07	.7545	.35	.0977	.26	.2186	.29	.1692	.29	.1649
ADC	.31	.1453	.39	.0623	.57	.0040	.69	.0009	.50	.0133	.50	.0163
Fornix												
FA	.63	.0009	.57	.0067	.68	.0003	.74	.0004	.68	.0003	.61	.0037
ADC	.67	.0004	.61	.0035	.66	.0005	.77	.0002	.61	.0014	.61	.0033
Superior cingulum												
FA	.34	.1074	.33	.1140	.59	.0026	.50	.0158	.17	.4266	.16	.4429
ADC	.44	.0325	.50	.0169	.54	.0067	.51	.0154	.21	.3372	.24	.2549
Posterior cingulum												
FA	.07	.7336	.05	.8024	.19	.3734	.02	.9137	.23	.2814	.26	.2124
ADC	.13	.5512	.26	.2064	.29	.1763	.32	.1301	.35	.0980	.40	.0545
inferior cingulum												
FA	.36	.0817	.38	.0665	.47	.0217	.42	.0453	.49	.0149	.46	.0280
ADC	.22	.3129	.30	.1467	.20	.3429	.33	.1140	.17	.4336	.25	.2363
inferior long. fasciculus												
FA	.16	.4510	.08	.7167	.56	.0044	.37	.0750	.51	.0114	.44	.0367
ADC	.01	.9806	.07	.7355	.40	.0548	.46	.0265	.30	.1485	.29	.1675
Uncinate fasciculus												
FA	.29	.1778	.33	.1188	.65	.0006	.62	.0032	.40	.0531	.43	.0414
ADC	.41	.0477	.50	.0173	.63	.0010	.71	.0007	.44	.0298	.40	.0535

Correlations significant at the .05 level are in red; those meeting family-wise Bonferroni correction (p=.012, 1-tailed, α=.05, n=8) are in red and bold.

[a] Single regression.

[b] Spearman rank.

Table 6

Percentage variance in performance in Working Memory explained by age and selected DTI Metrics

Predictor	%variance	p value
Age	47.70	**.0003**
Genu FA	39.60	**.0010**
Fornix FA	39.90	**.0009**
Fornix ADC	44.60	**.0004**
Age after genu FA	8.30	.0822
Age after fornix FA	8.00	.0851
Age after fornix ADC	4.10	.2047
Age after all(n=3)	0.40	.7003
Genu FA after age	2.20	.3560
Fornix FA after age	2.20	.3498
Fornix ADC after age	3.00	.2754

Correlations significant at the .05 level are in red; those meeting family-wise Bonferroni correction (p=.025, 1-tailed, α=.05, n=4) are in red and bold.

Table 7

Percentage of variance in age-Working Memory relations attenuated by selected DTI metrics and variance in DTI metrics-WM relations attenuated by age

Predictor	% variance attenuated
Age attenuated by genu FA	81.84
Age attenuated by fornix FA	82.49
Age attenauted by fornix ADC	91.03
Age attenuted by all 3	99.12
Genu FA attentuated by age	94.44
Fornix FA attentuated by age	94.49
Fornix ADC attenuated by age	93.27

Table 8

Percentage of variance in performance in Motor explained by age and selected DTI metrics

Predictor	% Variance	*p* Value
Age	49.40	**.0001**
Genu FA	40.50	**.0008**
Genu ADC	45.40	**.0003**
Splenium ADC	32.00	**.0040**
Fornix FA	45.80	**.0003**
Fornix ADC	43.00	**.0005**
UF FA	42.50	**.0006**
UF FA/UF ADC	39.70	**.0010**
Age after genu FA	10.50	.0465
Age after genu ADC	7.50	.0748
Age after splenium ADC	20.30	**.0070**
Age after fornix FA	7.20	.0859
Age after fornix ADC	7.60	.0870
Age after UF FA	16.50	**.0085**
Age after UF ADC	12.70	.0275
Age after all(n=7)	7.90	.0243
Genu FA after age	1.60	.4240
Genu ADC after age	3.90	.2038
splenium ADC after age	2.60	.2760
Fornix FA after age	3.60	.2188
Fornix ADC after age	1.20	.4873
UF FA after age	9.60	.0378
UF ADC after age	3.00	.2624

Correlations significant at the .05 level are in red; those meeting family-wise Bonferroni correction (p=.012, 1-tailed, α=.05, n=8) are in red and bold.

Table 9

Percentage of variance in age - Motor relations attenuated by selected DTI metrics and variance in DTI metrics-MOT relations attenuated by age

Predictor	% variance attenuated
Age attenuated by genu FA	78.74
Age attenuated by genu ADC	84.01
Age attenuated by splenium ADC	58.91
Age attenuated by fornix FA	84.62
Age attenuated by fornix ADC	84.62
Age attenuated by UF FA	66.60
Age attenuated by UF ADC	74.29
Age attenuated by all 7	84.01
Genu FA attenuated by age	96.05
Genu ADC attenuated by age	91.41
Splenium ADC attenuated age	90.94
Fornix FA attenuated by age	92.14
Fornix ADC attenuated by age	97.91
UF FA attenuated by age	77.41
UF ADC attenuated by age	92.44

Table 10

Percentage of variance in performance in Working Memory explained by age and selected DTI Metrics

Predictor	% Variance	*p* Value
Age	57.00	**.0001**
Genu FA	36.00	**.0019**
Genu ADC	44.60	**.0004**
Fornix FA	45.80	**.0003**
Fornix ADC	37.70	**.0014**
Age after genu FA	22.40	**.0043**
Age after genu ADC	12.70	.0153
Age after fornix FA	12.60	.0197
Age after fornix ADC	19.80	**.0014**
Age after all (n=4)	2.20	.3268
Genu FA after age	1.40	.9731
Genu AD after age	0.30	.4046
Fornix FA after age	1.40	.3983
Fornix ADC after age	0.50	.6984

Correlations significant at the .05 level are in red; those meeting family-wise Bonferroni correction (*p*=.025, 1-tailed, *α*=.05, *n*=4) are in red and bold.

Table 11

Percentage of variance in age -Problem Solving relations attenuated by selected DTI metrics and variance in DTI metrics and variance in DTI metrics-PS relations attenuated by age

Predictor	% variance attenuated
Age attenuated by genu FA	60.70
Age attenuated by genu AADC	77.72
Age attenuated by fornix FA	77.89
Age attenuated by fornix ADC	65.26
Age attenuated by all	96.14
Genu FA attenuated by age	96.11
Genu ADC attenuated by age	99.33
Fornix FA attenuated by age	96.94
Fornix ADC attenuated by age	98.67